Mincyt CIENCIA EN REVOLUCIÓN CNTQ

*Grima et al*, Vol. 7, Nro. 21, 37–45, mayo–agosto, 2021.

Article:

# Synthesis, X-Ray Diffraction, Scanning Electron Microscopy, Differential Thermal Analysis and Magnetic Susceptibility of the alloy $(CuAlSe_2)_{1-x}(TaSe)_x$ with $x = 0.5$

P. Grima-Gallardo[1,2,3*], A. Velásquez[2,3], G.E. Delgado[4] E. Pérez-C.[5],

[1]Centro de Estudios en Semiconductores, Departamento de Física, Facultad de Ciencias, Universidad de Los Andes, Mérida, Venezuela

[2]Centro Nacional de Tecnologías Ópticas, Mérida, Venezuela

[3]Centro de Investigaciones de Astronomía, Mérida, Venezuela

[4]Laboratorio de Cristalografía, Departamento de Química, Facultad de Ciencias, Universidad de Los Andes, Mérida, Venezuela

[5]Instituto de Ciencia y Tecnología de Materiales, Universidad de La Habana, Vedado, Cuba

Recibido: mayo 2021
Aceptado: julio 2021
Autor para correspondencia: P. Grima-G. e–mail: peg1952@gmail.com
DOI: https://doi.org/10.5281/zenodo.5721457

**Abstract**

Polycrystalline samples of the alloy $(CuAlSe_2)_{1-x}(TaSe)_x$ with $x = 0.5$ were prepared by the melt and anneal method and characterized by X-Ray Diffraction (XRD), Scanning Electron Microscopy (SEM), Differential Thermal Analysis (DTA), and Magnetic Susceptibility (MS) techniques. It was found that this alloy is composed of two main phases, one poor and another rich in Ta, and traces of $TaSe_2$. The sample shows a weak ferromagnetic behavior with $T_c > 300$ K, a characteristic that can be useful for room-temperature ferromagnetic devices.

**Keywords:** semiconductors; alloys, crystal structure, RT-ferromagnetism.

Artículo:

# Síntesis, difracción de rayos X, microscopía electrónica de barrido, análisis térmico diferencial y susceptibilidad magnética de la aleación $(CuAlSe_2)_{1-x}(TaSe)_x$ con $x = 0.5$

**Resumen**

Muestras policristalinas de la aleación $x = 1/2$ del sistema $(CuAlSe_2)_{1-x}(TaSe)_x$ fueron preparadas por el método de fusión y recocido, caracterizándolas por las técnicas de Difracción de Rayos X (DRX), Microscopía Electrónica de Barrido (MEB), Análisis Térmico Diferencial (ATD) y Susceptibilidad Magnética (SM). Se encontró que las muestras contienen dos fases principales, una pobre y otra rica en Ta, y trazas de $TaSe_2$. La muestra presenta un comportamiento ferromagnético débil con $T_c > 300$ K, característica que puede ser útil para dispositivos ferromagnéticos a temperatura ambiente.

**Palabras claves:** semiconductores; aleaciones; estructura cristalina; ferromagnetismo a temperatura ambiente.

# 1 Introduction

(I-III-$VI_2$)/(TM-VI) alloys have been studied in recent years [1]-[26] to create new materials for spintronics and room temperature ferromagnetism applications, in analogy with parent II-IV-$V_2$/III-V alloys [28]-[37]. In addition, an unusual superconductor behavior observed in $CuCo_2InS_4$ [25] and $CuInNbTe_3$ [26] has opened a new research perspective for these alloys.

The substitution of I or III cation by a TM-atom in the cationic sublattice of the ordered chalcopyrite crystal structure of I-III-$VI_2$ compounds (space group $I\bar{4}2d$) produce a gradual disorder that induces a structural transition to the semi-ordered chalcopyrite-like structure (space group $P\bar{4}2c$). This gradual crystal structure transition takes place during a large composition range.

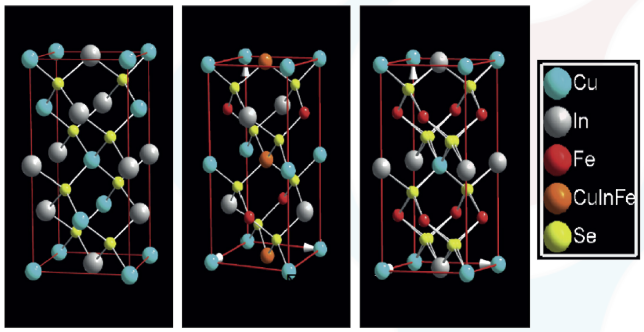


Figure 1: Structural phase transitions for (I-III-$VI_2$)$_{1-x}$(TM-VI)$_x$ alloys. For better comprehension $(CuInSe_2)_{1-x}(FeSe)_x$ alloys have been taken as an example. At the left side of the figure, the ordered chalcopyrite structure of $CuInSe_2$. At the center, the semiordered chalcopyrite-like structure, for compositions $0 < x < 2/3$; the orange atom represents the crystallographic site which is shared by the three cations. On the right side, the reordered stannite structure; observe the TM layers

(I-III-$VI_2$)/(TM-VI) alloys can be represented by the equation (I-III-$VI_2$)$_{1-x}$(TM-VI)$_x$ where $x$ is the composition range. If that is the case, for $x = 2/3$, the number of TM-atoms equals the number of I and III-atoms. It had been observed that, at this composition value, a new reordering occurs [21, 22, 23], then, the $P\bar{4}2c$ structure transits to the ordered stannite $I\bar{4}2d$ crystal structure. Figure 1 is a representation of the crystal structure sequence, taken $(CuInSe_2)_{1-x}(FeSe)_x$ alloys as an example.

An exception to this general behavior has been observed in alloys where Ta is the TM-atom. In the $(CuAlSe_2)_{1-x}(TaSe)_x$ and $(CuGaSe_2)_{1-x}(TaSe)_x$ alloy systems, an intermediate hexagonal phase (space group ) analogous to the $Cu_{0.52}TaSe_2$ phase but with the Cu site shared with Al (Ga), merges at $x > 0.2$ due to the low solubility of Ta in the ternary alloy [22, 23, 24]. (Cu-III)$_{0.5}TaSe_2$ (III: Al, Ga) phases are topological 2D-layer types and can be defined as a $TaSe_2$-like phase. $TaSe_2$ is a rather complex system, with many polytypic forms. It has been investigated due to the interest because of the presence of charge density wave phenomena (CDW) encountered in this compound [27].

From the magnetic point of view, I-III-$VI_2$ compounds are diamagnetic; the exchange of I and/or III-atoms for TM-atoms in the ternary chalcopyrite matrix induces a variety of magnetic effects. Because of their electronic structure (Ar $3d^5$ $4s^2$), $Mn^{2+}$ has been used extensively as TM for (I-III-$VI_2$)/(TM-VI) alloys; at low concentrations (less than 5 %) Mn substitution is paramagnetic with a little coupling of $Mn^{2+}$ moments but at higher $Mn^{2+}$ concentration appears antiferromagnetic coupling [38, 39, 40]. However, for the $CuGaTe_2$/MnTe system, the magnetic character could be accounted for the formation of $Mn^{2+}$-containing superparamagnetic clusters [41] corroborated by EPR measurements [14]. A similar superparamagnetic behavior has been observed in Cu(In,Ga)$FeTe_3$ [42], $(CuInSe_2)_{1-x}(TaSe)_x$ [43], $(CuGaSe_2)_{1-x}(TaSe)_x$ [24], $(CuAlSe_2)_{1-x}(TaSe)_x$ [22] and $(CuInTe_2)_{1-x}(TaTe)_x$ [44] alloy systems.

In this work, we are reporting the synthesis and characterization of the alloy $x = 1/2$ that belongs to the $(CuAlSe_2)_{1-x}(TaSe)_x$ alloy system with emphasis on the identification of the intermediate hexagonal phase and the magnetic behavior.

# 2 Experimental Procedure

## 2.1 Synthesis

Samples have been produced by the melt and anneal method as is described below. Starting materials (Cu, Al, Ta, and Te with nominal purity of

99.99 wt. %) in the stoichiometric ratio were mixed in an evacuated ($10^{-4}$ Torr) and sealed quartz tube with the inner walls previously carbonized to prevent the chemical reaction of the elements with quartz. The ampoule was heated until 490 K (melting point of Se) keeping this temperature for 48 h and shaking all the time using an electromechanical motor. This procedure guarantees the formation of binary species at low temperatures avoiding the existence of free Se at high temperatures, which could produce Se deficiency in the ingot. Then the temperature was slowly increased until 1423 K, with the mechanical shaker always connected for better mixing of the components. After 24 h, the cooling cycle begins descending the temperature down to 800 K (the annealing temperature) with the mechanical shaker off. The ampoule is keeping at the annealing temperature for 30 days to guarantee a good thermal equilibrium for X-ray diffraction measurements and then the furnace is switching off to room temperature.

## 2.2 X-Ray Diffraction (XRD)

X-ray powder diffraction data were collected employing a diffractometer (Siemens D5005) equipped with a graphite monochromator ($CuK_\alpha$, $\lambda = 1.54059$ Å) at 40 kV and 20 mA. Silicon powder was used as an external standard. The samples were scanned from 10 – 100° $2\theta$, with a step size of 0.02° and a counting time of 20 s. The Bruker analytical software was used to establish the positions of the peaks from the $CuK\alpha_2$ component and to strip mathematically the $CuK\alpha_1$ components from each reflection. The peak positions were extracted employing a single-peak profile fitting carried out through the Bruker DIFFRACplus software. Each reflection was modeled utilizing a pseudo-Voigt function.

## 2.3 Scanning Electron Microscopy (SEM)

Stoichiometric relations were investigated by scanning electron microscopy (SEM) technique, using Hitachi S2500 equipment. The microchemical composition was found by an energy-dispersive x-ray spectrometer (EDS) coupled with a computer-based multichannel analyzer (MCA, Delta III analysis, and Quantex software, Kevex). For the EDS analysis, $K_\alpha$ lines were used. The accelerating voltage was 15 kV. The samples were tilted 35 degrees. A standardless EDS analysis was made with a relative error of $\pm(5-10)\%$ and detection limits of the order of 0.3 wt %, where the k-ratios are based on theoretical standards.

## 2.4 Differential Thermal Analysis (DTA)

Differential Thermal Analysis (DTA) measurements were carried out in a fully automatic Perkin-Elmer apparatus, which consists of a Khantal resistance furnace ($T_{max} = 1650$ K) equipped with Pt/Pt-Rh thermocouples and an informatics system for the automatic acquisition data. The internal standard used was a high purity (99.99 wt. %) piece of gold. The temperature runs have been performed from ambient temperature to 1400-1500 K, which is the recommended operative limit. The heating rate was controlled electronically to 20 $Kh^{-1}$; the cooling rate was given by the natural cooling of the furnace after switching off. Transition temperatures were manually obtained from the $\Delta T$ vs. T graph with the criteria that the transition occurs at the intersection of the baseline with the slope of the thermal transition peak. The maximum error committed in the determination of transition temperatures by this method was estimated to be ± 10 K.

## 2.5 Magnetic susceptibility

DC magnetic susceptibility as a function of temperature measurements, $\chi(T)$, was performed on a Quantum Design SQUID magnetometer, equipped with a superconducting magnet able to produce fields up to 5 T. Samples in the form of powder were compacted with a piece of cotton inside the sample holder to prevent any movement. Zero-field-cooling and field cooling (ZFC-FC) measurements were carried out in the temperature range 2–300 K using the standard method of cooling the sample to the lowest temperature (usually 2 K) without applied magnetic field, then heating the sample to room temperature applying a little magnetic field

of 100–500 Oe, and finally cooling again to the minimum temperature.

## 3 Result Analysis and Discussion

In Figure 2, the experimental X-ray diffraction pattern for sample $x = 1/2$ (nominally $CuAlTaSe_3$) is presented. The analysis indicates that the pattern is composed of the following phases: a semi-ordered $P\bar{4}2c$ chalcopyrite-like (labels in red), a hexagonal $P\bar{6}m2$ $Cu_{0.52}TaSe_2$-like and traces of $TaSe_2$ (labels in green).

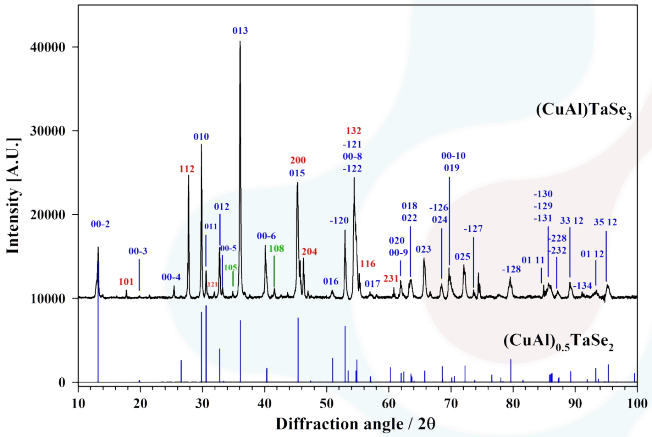


Figure 2: Sample diffraction pattern $x = 1/2$ (nominally $CuAlTaSe_3$). Numbers correspond to hkl-Miller indices: (red) Chalcopyrite-like, (blue) hexagonal $Cu_{0.52}TaSe_2$-like, and (green) traces of $TaSe_2$

The hexagonal phase has been compared with a calculated $(CuAl)_{0.5}TaSe_2$ structure show in Figure 2); the agreement between experimental and calculated is a very good suggesting that the Cu-atomic crystallographic sites are shared with Al, in analogy with the recently reported $(CuGa)_{0.52}TaSe_2$ phase [45]. Rietveld refinements are in course to quantify the occupation factor of Cu and Al in the 2i crystallographic site and will be reported in a specialized journal in the next future. A preliminary indexation using DICVOL06 software [46] gives lattice parameters values of $a = b = 3.455 \pm 0.002$, $c = 13.409 \pm 0.005$, $V = 139.7 \pm 1$ Å$^3$ for the hexagonal phase and $a = 5.606 \pm 0.001$ Å; $c = 10.904 \pm 0.03$ Å; $c/a = 1.94$; $V = 342.7 \pm 1$ Å$^3$ for the tetragonal phase.

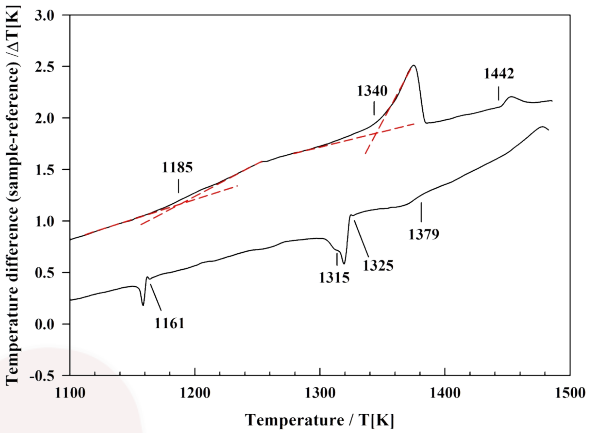


Figure 3: Sample thermogram $x = 1/2$ (nominally $CuAlTaSe_3$). The red dashed lines illustrate the method to obtain the thermal transition temperatures (the crossover of the baseline with the slope of the peak)

In the thermogram of Figure 3, in the heating cycle, the melting point was observed at 1442 K. The peak at 1340 K corresponds to a thermal transition of the type solid-solid + liquid, whereas the peak at 1185 K suggests a slow order-disorder transition. In the cooling cycle, the solidification point is observed at 1379 K, the solid + liquid-solid transition at 1325 K, and the disorder → order transition at 1161 K. The little shoulder at 1315 K indicates the presence of a narrow solid + liquid region.

The stoichiometry of the nominal sample $CuAlTaSe_3$ has been measured by scanning electron microscopy and is given in Table 1. The $CuAlS_2$-like phase contains $5.7 \pm 0.5$ % atoms of Ta, nearly equal quantities of Cu and Al ($19.3 \pm 0.3$ % and $19.7 \pm 0.3$ %) atoms, respectively) and $55.3 \pm 0.7$ % atoms of Se. According to the crystal structure observed by XRD and the measured stoichiometry by SEM, which can be written as $(CuAl)_{1.2}Ta_{0.3}Se_2$, this phase qualifies as a semi-ordered chalcopyrite-like structure with a low solubility of Ta ($< 10$ %) which is in agreement with previous experimental results observed in analogous alloy systems [22, 23, 43, 44]. The $(Cu_{0.52}TaSe_2)$-like phase contains $9.8 \pm 0.3$ % atoms of Cu, $7.0 \pm 0.5$ % atoms of Al,

Table 1: Measured stoichiometry of the alloy $(CuAlSe2)_{1-x}(TaSe)_x$ with $x = 0.5$

| Composition (x) | Molecular Weight (g/mol) | Nominal stoichiometry (% Atom) | | Experimental stoichiometry (% Atom) | |
|---|---|---|---|---|---|
| | | $CuAlS_2$-like phase | $(Cu_{0.52}TaSe_2)$-like phase | $CuAlS_2$-like phase | $(Cu_{0.52}TaSe_2)$-like phase |
| $x = 1/2$ | 249.18 | Cu = 16.67<br>Al = 16.67<br>Ta = 16.67<br>Se = 50.00 | Cu = 07.4<br>Al = 07.4<br>Ta = 28.4<br>Se = 56.8 | Cu = 19.3 ± 0.3<br>Al = 19.7 ± 0.3<br>Ta = 05.7 ± 0.5<br>Se = 55.3 ± 0.7 | Cu = 09.8 ± 0.3<br>Al = 07.0 ± 0.5<br>Ta = 29.8 ± 0.4<br>Se = 53.4 ± 0.6 |

$29.8 \pm 0.4$ % atoms of Ta, and $53.4 \pm 0.6$ % atoms of Se which is in good agreement with the calculated nominal stoichiometry for this phase. The Cu atoms represent 58.3 % and Al the 41.7 % of the atoms in the 2i site, in consequence, the stoichiometry of the sample can be written as $(Cu_{0.30}Al_{0.22})TaSe_2$.

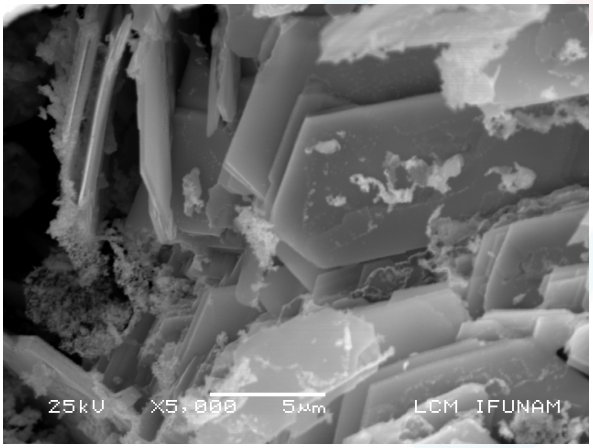


Figure 4: Microphotography of the hexagonal $Cu_{0.30}Al_{0.22}TaSe_2$ phase

The microphotography of the $(Cu_{0.30}Al_{0.22})TaSe_2$ phase in Figure 4 shows the 2D-laminar character of this phase, characteristic of other Ta-rich phases [22].

Finally, in Figure 5, the mass magnetic susceptibility of sample $x = 1/2$ is displayed. The sample is a weak ferromagnetic with a critical temperature $T_c > 300$ K. The hystereses between ZFC and FC curves evidence the presence of magnetic nanoclusters. An additional magnetic contribution at low temperature, for $T < 27$ K, is due to the size of the nanoclusters. In the temperature interval, $2 < T < 27$ K, the nanoclusters unblock at

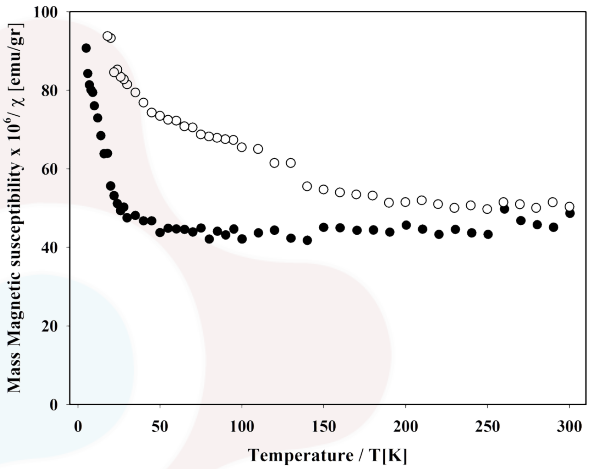


Figure 5: Mass magnetic susceptibility of sample $x = 1/2$ f of the $(CuAlSe_2)_{1-x}(TaSe)_x$ alloy system

different temperatures depending on their size up to $T \sim 27$ K where all the nanoclusters are unblocked. It is not possible, at the stage of this investigation, to elucidate the contribution of each of the two phases in the alloy; the chalcopyrite-like phase has a much less amount of Ta than the hexagonal phase, in consequence, their contribution must be less important. The preparation of the hexagonal $Cu_{0.30}Al_{0.22}TaSe_2$ phase will be a task in the next future.

## 4 Conclusions

Polycrystalline samples with $x = 1/2$ of the $(CuAlSe_2)_{1-x}(TaSe)_x$ alloy system have been synthesized and characterized by XRD, DTA, SEM, and MS techniques. It was found that the samples contain two main phases, one poor and another rich

in Ta, $(CuAl)_{1.2}Ta_{0.3}Se_2$ and $(Cu_{0.30}Al_{0.22})TaSe_2$ respectively, and traces of $TaSe_2$. The sample shows a weak ferromagnetic behavior with $T_c > 300$ K, a characteristic that can be useful for room-temperature ferromagnetic devices.

## Acknowledgments

We are very grateful to Dr. Dwight Acosta, Institute of Physics, Universidad Autónoma de México (UNAM) for SEM measurements.

## References

[1] L.J. Lin, N. Tabatabaie, J.H. Wernick, G.W. Hull, and B. Meagher. Optical, Electronic and Magnetic Properties of the Dilute Magnetic Semiconductor Mn:$CuInTe_2$. *Journal of Electronic Materials*, 17:321–324, 1988.

[2] P.M. Shand, P.A. Polstra, I. Miotkowski, and B.C. Crooker. Magnetic Dehavior of $CuIn_{1-x}Mn_{2x}Te_2$. *Journal of Applied Physics*, 75:5731–5733, 1994.

[3] N. Tsuji, H. Kitazawa, and G. Kido. Electric and Magnetic Properties of Mn- and Fe- Doped $CuInS_2$ Compounds. *Physics Status Solidi*, 189:951–954, 2002.

[4] T. Katamani and H. Akai. Magnetic Properties of Chalcopyrite-Based Diluted Magnetic Semiconductors. *Journal of Superconductivityl*, 16(1):95–97, 2003.

[5] T. Katamani and H. Akai. The Magnetic Properties in Transition Metal-Doped Chalcopyrite Semiconductors. *Materials Science in Semiconductor Processing*, 6:389–301, 2003.

[6] Y.-J. Zhao and A. Zunger. Electronic Structure and Ferromagnetism of Mn-Substituted $CuAlS_2$, $CuGaS_2$, $CuInS_2$, $CuGaSe_2$ and $CuGaTe_2$. *Physical Review B: Condensed Matter and Materials Physics*, 69:104422, 2004.

[7] Y.-J. Zhao and A. Zunger. Site Preference for Mn Substitution in Spintronic $Cu^{miii}x_2{}^{vi}$ Chalcopyrite Semiconductors. *Physical Review B: Condensed Matter and Materials Physics*, 69:075208, 2004.

[8] S. Schorr, M. Tovar, N. Stü$\beta$er, and K. Bente. Investigation of Structural Anomaly and Metal Ordering in the Solid Solution 2ZnS-$CuInS_2$ by Neutron Diffraction. *Physica B: Condensed Matter*, 350:e411–e414, 2004.

[9] S. Schorr, R. Höehne, G. Warner, V. Riede, and W. Kockelmann. Investigation of the Solid Solution Series 2(MnX)-$CuInX_2$ (X = S, Se). *Journal of Physics and Chemistry of Solids*, 66:1966–1969, 2005.

[10] S. Schorr, R. Höehne, D. Spemann, Th. Doering, and B.V. Korzun. Magnetic Properties Investigations of Mn Substituted $ABX_2$ Chalcopyrites. *Physica Status Solidi (a): Applications and Materials Science*, 203:2783–2787, 2006.

[11] S. Schorr, M. Tovar, N. Stuesser, D. Sheptyakov, and G. Geandier. Where the Atoms Are: Cation Disorder and Anion Displacement in $D^{II}X^{VI}$–$A^{I}B^{III}X^{VI}_2$ Semiconductors. *Physica B: Condensed Matter*, 385–386(Part 1):571–573, 2006.

[12] A. Pietnoczka, R. Bacewicz, and S. Schorr. Local Structure in $(MnS)_{2x}(CuInS_2)_{1-x}$ Alloy. *Physica Status Solidi (a): Applications and Materials Science*, 203(11):2746–2750, 2006.

[13] V.M. Novotortsev, G.G. Shabuninab, L.I. Koroleva, T.G. Aminov, R.V. Demin, and S.B. Boichuk. Superparamagnetism in Mn-Doped $CuGaTe_2$. *Inorganic Materials*, 43:12–17, 2007.

[14] J. Pérez, P.J. Silva, C.A. Durante-Rincón, J. Primera-Ferrer, and J.R. Fermín. EPR Study of the Diluted Magnetic Semiconductor $CuGa_{1-x}Mn_xTe_2$. *Journal Magnetism and Magnetic Materials*, 320:2155–2158, 2008.

[15] P. Grima-Gallardo, E. Calderón, M. Muñoz-Pinto, S. Durán-Piña, M. Quintero, E. Quintero, M. Morocoima, G.E. Delgado, H. Romero, J.M. Briceño, and J. Fernández. Synthesis and Characterization of $Cu_3TaIn_3Se_7$ and

$CuTa_2InTe_4$. *Physica Status Solidi (a): Applications and Materials Science*, 205(7):1552–1559, 2008.

[16] J. Yao, N. Kline, H. Gu, M. Yan, and J.A. Aitken. Effects of Mn Substitution on the Structure and Properties of Chalcopyrite-Type $CuInSe_2$. *Journal Solid State Chemistry*, 182:2579–2586, 2009.

[17] J. Yao, C.D. Brunetta, and J.A. Aitken. Suppression of Antiferromagnetic Interactions Through Cu Vacancies in Mn-Substituted $CuInSe_2$ Chalcopyrites. *Journal Physics: Condensed Matter*, 24(8):086006, 2012.

[18] P. Grima-Gallardo, O. Izarra, R. Peña, M. Muñoz, S. Durán, M. Quintero, E. Quintero y H. Romero. Comportamiento magnético de la aleación $(CuInTe_2)_{1-x}(TaTe)_x$ con $x = 0.25$. *Revista Cubana de Física*, 32(1):18–25, 2015.

[19] J. Yao, B.W. Rudyk, C.D. Brunetta, K.B. Knorr, H.A. Figore, A. Mar, and J.A. Aitken. Mn Incorporation in $CuInS_2$ Chalcopyrites: Structure, Magnetism, and Optical Properties. *Materials Chemistry and Physics*, 136(2-3):415–423, 2012.

[20] S. Torres-Cuenza, P. Grima-Gallardo, M. Muñoz, S. Durán, M. Quintero, L. Nieves y R.Tovar. Magnetic Behavior of the Alloy $(CuInSe_2)_{1-x}(FeSe)_x$ with $x = 0.5$. *Acta Científica Venezolana*, 66(1):56–59, 2015.

[21] P. Grima-Gallardo, S. Torres, M. Quintero, L. Nieves, E. Moreno, and G.E. Delgado. Phase Diagram of $(CuInSe_2)_{1-x}(FeSe)_x$ Alloys. *Journal of Alloys and Compounds*, 630:146–150, 2015.

[22] S. Torres-Cuenza, P. Grima-Gallardo, M. Muñoz, S. Durán, M. Quintero, L. Nieves y R. Tovar. Magnetic Dehavior of the Alloy $(CuInSe_2)_{1-x}(FeSe)_x$ with $x = 0.5$. *Acta Científica Venezolana*, 66(1):56–59, 2015.

[23] P. Grima-Gallardo, S. Durán, M. Muñoz, D.P. Rai, and G.E. Delgado. $(Cu_{0.4}Al_{0.3})TaSe_2$: Preparation and Crystal Structure Analysis from X-ray Powder Diffraction. *Southern Brazilian Journal of Chemistry*, 28(29):1–6, 2020.

[24] P. Grima-Gallardo, M. Muñoz, S. Durán, G.E. Delgado, E. Pérez-Cappé, and J.A. Aitken. X-ray Diffraction, Scanning Electron Microscopy and Differential Thermal Analysis of $(CuGaSe_2)_{1-x}(TaSe)_x$ Alloys System ($0 \leq x \leq 0.5$). *Senhri Journal of Multidisciplinary Studies*, 5(1):1–18, 2020.

[25] P. Grima-Gallardo, G.E. Delgado, E. Pérez-Cappé, J.A. Aitken y D.P. Rai. Synthesis, X-ray Diffraction, and Magnetic Measurements of $Cu(Ni,Co)InS_4$ Alloys: Superconductor Behavior of $CuCo_2InS_4$. *Revista LatinoAmericana de Metalurgia y Materiales*, 40(2):131–141, 2020.

[26] P. Grima-Gallardo, M. Palmera, M. Muñoz, S. Durán, M. Quintero, E. Quintero, L. Nieves, E. Moreno, M.A. Ramos, and H. Romero. Superconductivity Observation in a $(CuInTe_2)_{1-x}(NbTe)_x$ Alloy with $x = 0.5$. *Advanced Materials Science and and Technology*, 7(2):1–11, 2013.

[27] M.-L. Doublet, S. Remy, and F. Lemoigno. Density Functional Theory Analysis of the Local Chemical Bonds in the Periodic Tantalum Dichalcogenides $TaX_2$ (X = S, Se, Te). *Journal of Chemical Physics*, 113(4):5879–5890, 2000.

[28] A.J. Freeman and Y.-J. Zhao. Advanced Tetrahedrally-Bonded Magnetic Semiconductors for Spintronic Applications. *Journal of Physics and Chemistry of Solids*, 64(9–10):1453–1459, 2003.

[29] G.A. Medvedkin, T. Ishibashi, T. Nishi. K. Hayata, Y. Hasewaga, and K. Sato. Room-Temperature Ferromagnetism in Novel Diluted Magnetic Semiconductor $Cd_{1-x}Mn_xGeP_2$. *Japanese Journal of Applied Physics*, 39:L949, 2000.

[30] S. Cho, S. Choi, G.-B Cha, S.C. Hong, Y. Kim, Yu-J Zhao, A.J. Freeman, J.B. Ketterson, B.J. Kim, Y.C. Kim, and B.Ch. Choi. Room-Temperature Ferromagnetism in $(Zn_{1-x}Mn_x)GeP_2$ Semiconductors. *Physics Review Letters*, 88:257203, 2002.

[31] S. Cho, J. Cho, S.C. Hong, and S. Cho. Mn-doped $ZnGeAs_2$ and $ZnSnAs_2$ Single Crystals: Growth, Electrical, and Magnetic Properties. *Journal of the Korean Physical Society*, 42:S739–S741, 2003.

[32] R.V. Demin, L.I. Koroleva, S.F. Marenkin, S. Mikhailov, T. Aminov, R. Szymczak, and M. Baran. Room-Temperature Ferromagnetism in Mn-Doped $CdGeAs_2$ Chalcopyrite. *Journal Magnetism and Magnetic Materials*, 290–291(Part 2):1379–1382, 2005.

[33] L.I. Koroleva, V.Yu. Pavlov, D.M. Zashchirinskiĭ, S.F. Marenkin, S.A. Varnavskiĭ, R. Szymczak, V. Dobrovol'skiĭ and L. Killinskiĭ. Magnetic and Electrical Properties of the $ZnGeAs_2$: Mn Chalcopyrite. *Physics of the Solid State*, 49:2121–2125, 2007.

[34] L. Kilanski, K. Szalowski, R. Szymczak, M. Górska, E. Dynowska, P. Aleshkevych, A. Podgórni, A. Avdonin, W. Dobrowolski, I. Fedorchenko, and S. Marenkin. $Zn_{1-x}(Mn,Co)_xGeAs_2$ Ferromagnetic Semi-Conductor: Magnetic and Transport Properties. *Acta Physica Polonica A*, 114(5):1151–1157, 2008.

[35] A. Kochura, R. Laiho, A. Lashkul, E. Lähderanta, M. Shakhov, I. Zakharov, S. Marenkin, A. Molchanov, S. Mikhailov, and G. Jurev. Synthesis and Magnetic Properties of Mn-doped $Cd_{0.1}Zn_{0.9}GeAs_2$ Solid Solutions. *Journal of Physics: Condensed Matter*, 20(23):335220, 2008.

[36] L. I. Koroleva, D. M. Zashchirinskiĭ, T. M. Khapaeva, S. F. Marenkin, I. V. Fedorchenko, R. Szymczak, B. Krzumanska, V. Dobrovol'skiĭ, and L. Kilanskiĭ. Manganese-doped $ZnSiAs_2$ chalcopyrite: A new advanced material for spintronics. *Physics Solid State*, 51:303–308, 2009.

[37] V.M. Novotortsev, A.V. Kochura, and S.F. Marenkin. New Ferromagnetics Based on Manganese-Alloyed Chalcopyrites $A^{II}B^{IV}C_2^V$. *Inorganic Materials*, 46:1421–1436, 2010.

[38] L.-J. Lin, N. Tabatabaie, J.H. Wernich, G.W. Hull, and B. Meager. Optical, Electronic and Magnetic Properties of the Dilute Magnetic Semiconductor Mn:$CuInTe_2$. *Journal of Electronic Materials*, 17:321–324, 1988.

[39] P.M. Shand, P.A. Polstra, I. Miotkowski and B.C. Crooker. Magnetic Behavior of $(CuIn)_{1-x}Man_{2x}Te_2$. *Journal Applied Physics*, 75(10):5731–5733, 1994.

[40] S. Schorr, R. Höehne, D. Spemann, Th. Doering, and B.V. Korzun. Magnetic Properties Investigations of Mn Substituted $ABX_2$ Chalcopyrites. *Physica Status Solidi (a): Applications and Materials Science*, 203(11):2737–2787, 2006.

[41] V.M. Novotortsev, G.G. Shabubina, L.I. Koroleva, T.G. Aminov, R.V. Demin, and S.V. Boichuk. Superparamagnetism in Mn-$CuGaTe_2$. *Inorganic Materials*, 43(1):12–17, 2007.

[42] P. Grima-Gallardo, F. Alvarado, M. Muñoz, S. Durán, M. Quintero, L. Nieves, E. Quintero, R. Tovar, M. Morocoima, and M.A. Ramos. Superparamagnetism in $CuFeInTe_3$ and $CuFeGaTe_3$. *Physica Status Solidi (a): Applications and Materials Science*, 209(6):1141–1143, 2012.

[43] P. Grima-Gallardo, L. Méndez, G.E. Delgado, H. Cabrera, E. Pérez-Cappé, I. Zumeta-Dubé, A. Rodríguez, J.A. Aitken, and D.P. Rai. $(CuInSe_2)_{1-x}$ $(TaSe)_x$ Solid Solutions ($0 < x \leq 0.5$): X-Ray Diffraction, Scanning Electron Microscopy, Differential Thermal Analysis and Magnetic Susceptibility. *International Journal Experimental Spectroscopic Technnology*, 3:016, 2018.

[44] P. Grima-Gallardo, O. Izarra, L. Mendez, S. Torres, M. Quintero, H. Cabrera, E. Pérez-Cappé, I. Zumeta-Dubé, A. Rodríguez, J.A. Aitken and D.P. Rai. Preparation and Characterization of $(CuInTe_2)_{1-x}(TaTe)_x$ Solid Solutions ($0 < x < 1$). *Journal of Alloys and Compounds*, 747:178–188, 2018.

[45] G.E. Delgado, S. Durán, J.A. Aitken, M. Muñoz, and P. Grima-Gallardo. The Crystal Structure of the New Layered Alloy $(CuGa)_{0.52}TaSe_2$ Studied by SEM, DTA, and XRPD. *Orbital: The Electronic Journal of Chemistry*, In press, 2021.

[46] A. Boultif and D. Louer. Powder Pattern Indexing with the Dichotomy Method. *Journal of Applied Crystallography*, 37:724–731, 2004.